

## Single-Molecule Redox Blinking of Perylene Diimide Derivatives in Water

Thorben Cordes,<sup>†,‡</sup> Jan Vogelsang,<sup>†,§</sup> Milena Anaya,<sup>||</sup> Carla Spagnuolo,<sup>||</sup> Andreas Gietl,<sup>†</sup> Wolfram Summerer,<sup>†</sup> Andreas Herrmann,<sup>⊥</sup> Klaus Müllen,<sup>||</sup> and Philip Tinnefeld<sup>\*†</sup>

*Angewandte Physik—Biophysik, and Center for NanoScience (CeNS), Ludwig-Maximilians-Universität München, Amalienstrasse 54, D-80799, München, Germany, Max-Planck-Institut für Polymerforschung, Ackermannweg 10, D-55128 Mainz, Germany, and Department of Polymer Chemistry, Zernike Institute for Advanced Materials, University of Groningen, Nijenborgh 4, 9747 AG Groningen, Netherlands*

Received November 25, 2009; E-mail: philip.tinnefeld@lmu.de

**Abstract:** Dynamic developments in ultrasensitive and superresolution fluorescence microscopy call for improved fluorescence markers with increased photostability and new functionalities. We used single-molecule spectroscopy to study water-soluble perylene dicarboximide fluorophores (PDI), which were immobilized in aqueous buffer by attaching the fluorophore to DNA. Under these conditions bright fluorescence, comparable to that of single-molecule compatible organic fluorophores, is observed with homogeneous spectral and fluorescence decay time distributions. We additionally show how the fluorescence of the PDI can be controlled through photoinduced electron-transfer reactions by using different concentrations of reductants and oxidants, yielding either blinking or stable emission. We explain these properties by the redox potentials of PDI and the recently introduced ROXS (reducing and oxidizing system) concept. Finally, we evaluate how this fluorescence control of PDIs can be used for superresolution “Blink-Microscopy” in aqueous or organic media and more generally for single-molecule spectroscopy.

The use of fluorescence microscopy in life sciences and nanotechnology has increased tremendously during the past decades, and a great variety of experimental techniques is currently available for the characterization of biological or artificial (nano)structures. Simultaneously, methods have been established that utilize fluorescence emission for an observation of single particles or (bio)molecules, that is, single-molecule fluorescence spectroscopy (SMFS).<sup>1–3</sup> These techniques recently merged in far-field superresolution approaches that are based on the subsequent localization of single molecules.<sup>4–6</sup> While technical developments are proceeding rapidly, most of the current approaches place additional demands on fluorophore design. Accordingly, modern fluorescence microscopy tech-

niques require bright (high extinction coefficient at the excitation wavelength, high fluorescence quantum yield), photostable, water-soluble, chemically compatible, nonperturbing, or even (photo-)switchable labels.<sup>7</sup>

Hitherto, predominantly fluorophores from the classes of (carbo)rhodamines, oxazines, cyanines, and DCDHF fluorophores<sup>8</sup> have been employed in biomolecular single-molecule studies or superresolution microscopy. On the other hand, rylene derivatives have been used for single-molecule spectroscopy since the early days.<sup>9</sup> Dyes such as perylene, perylene (di)imide, and others have proven to be bright and photostable fluorophores, well-suited for a multitude of important single-molecule studies.<sup>10–12</sup> In recent years, water-soluble and monofunctional derivatives of perylene and terylene dyes also have been developed<sup>13–17</sup> and were applied in first biomolecular single-

<sup>†</sup> Ludwig-Maximilians-Universität München.

<sup>‡</sup> Present address: Department of Physics and Biological Physics Research Group, Clarendon Laboratory, University of Oxford, Parks Road, Oxford OX1 3PU, U.K.

<sup>§</sup> Present address: Center for Nano and Molecular Science and Technology and Department of Chemistry and Biochemistry, The University of Texas at Austin, Austin, TX 78712.

<sup>||</sup> Max-Planck-Institut für Polymerforschung.

<sup>⊥</sup> University of Groningen.

- (1) Weiss, S. *Science* **1999**, *283*, 1676–1683.
- (2) Tinnefeld, P.; Sauer, M. *Angew. Chem., Int. Ed.* **2005**, *44*, 2642–2671.
- (3) Joo, C.; Balci, H.; Ishitsuka, Y.; Buranachai, C.; Ha, T. *Annu. Rev. Biochem.* **2008**, *77*, 51–76.
- (4) Betzig, E.; Patterson, G. H.; Sougrat, R.; Lindwasser, O. W.; Olenych, S.; Bonifacino, J. S.; Davidson, M. W.; Lippincott-Schwartz, J.; Hess, H. F. *Science* **2006**, *313*, 1642–1645.
- (5) Rust, M. J.; Bates, M.; Zhuang, X. *Nat. Methods* **2006**, *3*, 793–795.
- (6) Hess, S. T.; Girirajan, T. P.; Mason, M. D. *Biophys. J.* **2006**, *91*, 4258–4272.

(7) Hell, S. W. *Nat. Methods* **2009**, *6*, 24–32.

(8) Lord, S. J.; Conley, N. R.; Lee, H. L.; Nishimura, S. Y.; Pomerantz, A. K.; Willets, K. A.; Lu, Z.; Wang, H.; Liu, N.; Samuel, R.; Weber, R.; Semyonov, A.; He, M.; Twieg, R. J.; Moerner, W. E. *ChemPhys-Chem* **2009**, *10*, 55–65.

(9) Basche, T.; Moerner, W. E. *Nature* **1992**, *355*, 335–337.

(10) Hofkens, J.; Maus, M.; Gensch, T.; Vosch, T.; Cotlet, M.; Kohn, F.; Herrmann, A.; Mullen, K.; De Schryver, F. *J. Am. Chem. Soc.* **2000**, *122*, 9278–9288.

(11) Hofkens, J.; Cotlet, M.; Vosch, T.; Tinnefeld, P.; Weston, K. D.; Ego, C.; Grimsdale, A.; Muellen, K.; Beljonne, D.; Bredas, J. L.; Jordens, S.; Schweitzer, G.; Sauer, M.; De Schryver, F. *Proc. Natl. Acad. Sci. U.S.A.* **2003**, *100*, 13146–13151.

(12) Zurner, A.; Kirstein, J.; Dobliger, M.; Brauchle, C.; Bein, T. *Nature* **2007**, *450*, 705–708.

(13) Icli, S.; Demic, S.; Dindar, B.; Doroshenko, A. O.; Timur, C. *J. Photochem. Photobiol., A* **2000**, *136*, 15–24.

molecule studies.<sup>18,19</sup> Their photophysical characterization, however, lags behind, and single-molecule studies have generally been carried out in polymer matrices instead of physiologically relevant buffer conditions.<sup>20,21</sup> In other cases, fluorescence correlation spectroscopy was used that has a limited time range due to diffusion and does not reveal heterogeneity.<sup>14</sup>

In this paper, we used spectrally resolved and time-resolved single-molecule spectroscopy<sup>22</sup> to study the photophysics of water-soluble perylene diimide (PDI) dyes. For the first time, single PDI dyes were studied in aqueous buffer by attachment of the fluorophore to DNA and immobilization via streptavidin/biotin on bovine serum albumin (BSA-) coated cover slides. We found largely homogeneous photophysical properties of the PDIs with similar photostability as for other single-molecule-compatible fluorophores excitable at around 550 nm. We further demonstrated that the fluorescence properties of PDIs are largely dominated by their redox potentials in different buffer environments, that is, aqueous and organic media. Due to the low energy of the reduced state, blinking is easily induced and controllable in accordance with a concept involving a reducing and oxidizing system (ROXS).<sup>23–26</sup> Since the redox potentials of perylene derivatives can be controlled through suitable substituents at the chromophore,<sup>27</sup> our results pave the way for tailored photophysical properties that show the required emission for a specific application: Stable fluorescence or blinking could be adjusted at will for applications such as superresolution “Blink-Microscopy”.<sup>24,28</sup>

The investigated PDI derivative (Figure 1A) is water-soluble due to the presence of four aryl substituents bearing a sulfonic acid group. The fluorophore was coupled to a 38-mer single-stranded DNA (ssDNA; see Supporting Information for details) to facilitate the immobilization on glass surfaces via hybridization to a complementary strand that was bound to cover slides via BSA/biotin/streptavidin (see Supporting Information for the base composition of the ssDNA and the complementary

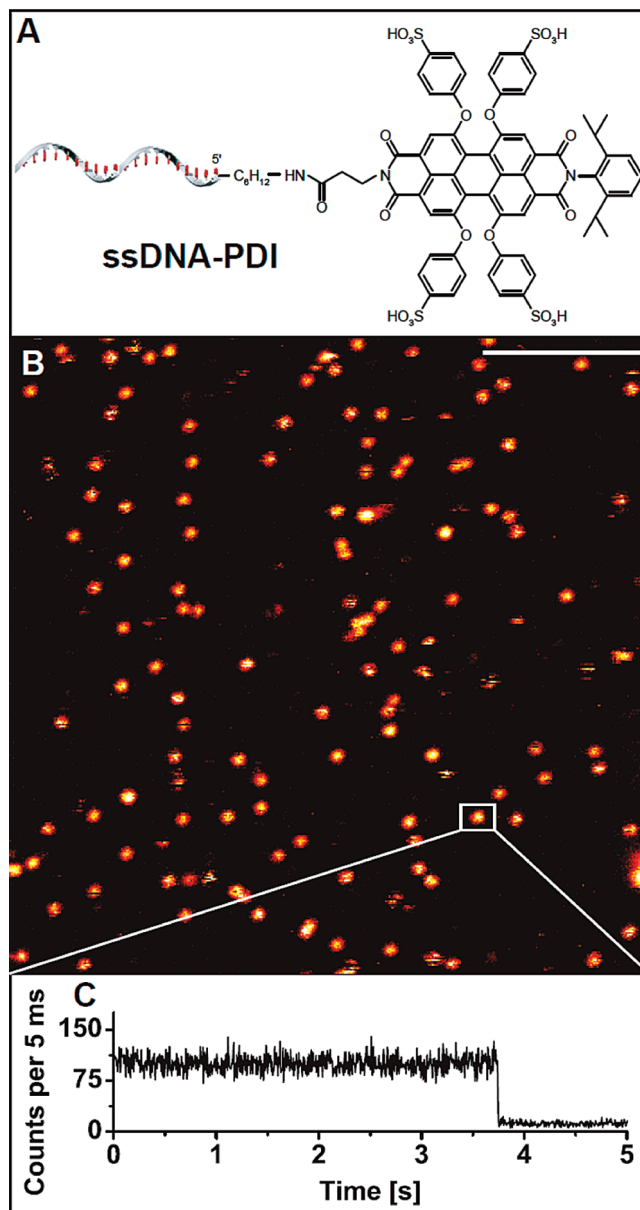


**Figure 1.** (A) Chemical structure of the PDI chromophore used. (B) Confocal fluorescence image of immobilized dsDNA–PDI in aqueous PBS buffer at pH = 7.4. The area shown ( $20 \times 20 \mu\text{m}$ , 2 ms/pixel, intensity scale from 10 to 120 counts/2 ms) was scanned by excitation at 560 nm with an average intensity of 3.8 kW/cm<sup>2</sup>. Scale bar at upper right is 5  $\mu\text{m}$ . (C) Fluorescence transient recorded under the same experimental conditions with no observable amplitude in the autocorrelation function down to 1  $\mu\text{s}$ . The image and the transient show the sum of both spectrally separated detection channels (for details see the Materials and Methods section in Supporting Information).

strand).<sup>23</sup> This immobilization strategy ensures that the fluorophores largely show the same properties as in free solution while they can be studied for an extended time compared to measurements of freely diffusing molecules.<sup>29</sup> The attachment of the chromophore<sup>14,15</sup> to the nucleic acid moiety was achieved by coupling the activated ester of the dye to the 5'-amino-modified DNA still bound to the solid support by employing the so-called “syringe synthesis technique” (for details see Supporting Infor-

- (14) Peneva, K.; Mihov, G.; Herrmann, A.; Zarrabi, N.; Borsch, M.; Duncan, T. M.; Mullen, K. *J. Am. Chem. Soc.* **2008**, *130*, 5398–5399.
- (15) Weil, T.; Abdalla, M. A.; Jatzke, C.; Hengstler, J.; Mullen, K. *Biomacromolecules* **2005**, *6*, 68–79.
- (16) Qu, J.; Kohl, C.; Potek, M.; Mullen, K. *Angew. Chem., Int. Ed.* **2004**, *43*, 1528–1531.
- (17) Peneva, K.; Mihov, G.; Nolde, F.; Rocha, S.; Hotta, J.; Braeckmans, K.; Hofkens, J.; Uji-i, H.; Herrmann, A.; Mullen, K. *Angew. Chem., Int. Ed.* **2008**, *47*, 3372–3375.
- (18) Samudrala, R.; Zhang, X.; Wadkins, R. M.; Mattern, D. L. *Bioorg. Med. Chem.* **2007**, *15*, 186–193.
- (19) Rocha, S.; Hutchison, J. A.; Peneva, K.; Herrmann, A.; Mullen, K.; Skjot, M.; Jorgensen, C. I.; Svendsen, A.; De Schryver, F. C.; Hofkens, J.; Uji-i, H. *ChemPhysChem* **2009**, *10*, 151–161.
- (20) Margineanu, A.; Hofkens, J.; Cotlet, M.; Habuchi, S.; Stefan, A.; Qu, J.; Kohl, C.; Muellen, K.; Vercammen, J.; Engelborghs, Y.; Gensch, T.; De Schryver, F. C. *J. Phys. Chem. B* **2004**, *108*, 12242–12251.
- (21) Jung, C.; Ruthardt, N.; Lewis, R.; Michaelis, J.; Sodeik, B.; Nolde, F.; Peneva, K.; Mullen, K.; Brauchle, C. *ChemPhysChem* **2009**, *10*, 180–190.
- (22) Tinnefeld, P.; Herten, D. P.; Sauer, M. *J. Phys. Chem. A* **2001**, *105*, 7989–8003.
- (23) Vogelsang, J.; Kasper, R.; Steinhauer, C.; Person, B.; Heilemann, M.; Sauer, M.; Tinnefeld, P. *Angew. Chem., Int. Ed.* **2008**, *47*, 5465–5469.
- (24) Vogelsang, J.; Cordes, T.; Forthmann, C.; Steinhauer, C.; Tinnefeld, P. *Proc. Natl. Acad. Sci. U.S.A.* **2009**, *106*, 8107–8112.
- (25) Cordes, T.; Vogelsang, J.; Tinnefeld, P. *J. Am. Chem. Soc.* **2009**, *131*, 5018–5019.
- (26) Cordes, T.; Stein, I. H.; Forthmann, C.; Steinhauer, C.; Walz, M.; Summerer, W.; Person, B.; Vogelsang, J.; Tinnefeld, P. *Proc. SPIE—Int. Soc. Opt. Eng.* **2009**, *7367*, 73671D.
- (27) Jones, B. A.; Facchetti, A.; Wasielewski, M. R.; Marks, T. J. *J. Am. Chem. Soc.* **2007**, *129*, 15259–15278.
- (28) Steinhauer, C.; Forthmann, C.; Vogelsang, J.; Tinnefeld, P. *J. Am. Chem. Soc.* **2008**, *130*, 16840–16841.

- (29) Okumus, B.; Wilson, T. J.; Lilley, D. M. J.; Ha, T. *Biophys. J.* **2004**, *87*, 2798–2806.

mation and Figures S1–S5).<sup>30</sup> A very good reaction yield of 73% was achieved.

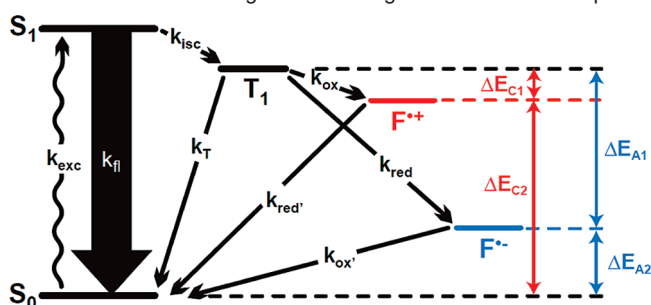
In water, the PDI exhibits a structured absorption with distinct bands in the visible and near-ultraviolet regions (see Figure S6 in Supporting Information). The lowest energy transition shows a maximum at 560 nm, while another transition is observed at ~425 nm. Fluorescence emission is red-shifted by 60 nm with a maximum at 620 nm.

For single-molecule measurements, we used a multicolor confocal setup equipped with a supercontinuum laser for free wavelength selection. Spectral information was obtained by splitting the fluorescence onto two spectrally separated detectors, and single-photon counting recording provided fluorescence lifetime information.<sup>22</sup> Surfaces were scanned via an *X/Y* piezo-stage over an area of  $20 \times 20 \mu\text{m}$ . Laser excitation at 560 nm ( $3.8 \text{ kW/cm}^2$ ) resulted in images such as that depicted in Figure 1B that shows the sum fluorescence of the two detectors (details of the experimental methods are described in Supporting Information). The diffraction-limited spots represented single immobilized PDI molecules in aqueous phosphate-buffered saline (PBS) at pH 7.4. The impression of reproducible fluorescence from single PDI molecules was further corroborated by the spectral and fluorescence lifetime images shown in Figure S7 in Supporting Information. Collecting all photons per spot by a spot-finding algorithm allowed creation of histograms of the fluorescence lifetime and the spectral properties that we discussed in terms of the fractional intensity on the long-wavelength detector [ $F_2$  value;  $F_2 = I_{\text{det}2}/(I_{\text{det}1} + I_{\text{det}2})$ ].<sup>22</sup> The histograms indicate narrow distributions of the photophysical properties of water-soluble PDIs on DNA, and no significant correlation between the photophysical parameters was observed (Figure S7C–E in Supporting Information). The mean fluorescence lifetime determined from the histogram was  $2.6 \pm 0.2 \text{ ns}$ .

For closer inspection, we placed single PDIs in the laser focus and studied their fluorescence as a function of time. For a considerable fraction (>60%) of molecules, transients similar to the one depicted in Figure 1C were obtained. These molecules showed stable emission of 20–30 kHz over a time scale of several seconds with rare and brief off-states. The signal in Figure 1C abruptly vanished after ~3.7 s where one-step photobleaching evidenced the observation of a single PDI molecule. These transients were further characterized by no noticeable amplitude in the autocorrelation function down to 1  $\mu\text{s}$ , since triplet states were efficiently depopulated by oxygen.<sup>31</sup> The remaining molecules showed more intensity fluctuations on different time scales or different intensity levels. We assume that these molecules represented a fraction of molecules where the local environment allowed more interactions, for example, with the BSA protein coating.

To quantify the photostability of the PDI under physiologically relevant condition we used total internal reflection (TIR) microscopy as described previously.<sup>23</sup> Here, 60 s movies with 100 ms integration time were recorded and the absolute number of active fluorophores per frame was analyzed by commercially available software (ImageJ 1.42).<sup>23</sup> The decreasing number of active fluorophores was then fitted by a single-exponential decay, resulting in a characteristic bleaching time. By considering the mean intensity of a single fluorophore per frame, the average

**Scheme 1.** Jablonski Diagram According to the ROXS Concept<sup>a</sup>



<sup>a</sup>  $S_0/S_1$ , electronic ground state and first excited singlet state;  $T_1$ , triplet state;  $F^-$  and  $F^+$ , reduced and oxidized states;  $k_{\text{exc}}$ , excitation rate;  $k_{\text{ri}}$ , emission rate;  $k_{\text{isc}}$ , rate of intersystem crossing;  $k_{\text{T}}$ , rate of triplet depletion;  $k_{\text{ox}}$  and  $k_{\text{red}}$ , oxidation and reduction rates. In the case of the investigated PDI derivative, the potentials of the ionized states are asymmetric with respect to  $E_{0,0}$  with estimated values  $E_{\text{red}} = -0.6 \text{ V}$  and  $E_{\text{ox}} = 1.4 \text{ V}$ .

detected photon number was  $44\,000 \pm 15\,000$  photons per molecule ( $\tau_{\text{bleach}} \sim 2.3 \pm 0.8 \text{ s}$ ;  $16 \text{ kW/cm}^2$  at 560 nm). Accordingly, PDI in aqueous buffer features good photostability and performance for single-molecule experiments better than other commonly used fluorophores in this spectral range.<sup>23</sup> For example, ATTO565, a fluorophore with comparable spectral properties, emits <10 000 photons under similar conditions.

Next, we studied whether we could control the photophysics of the PDI similar to other fluorophores using a reducing and oxidizing system (ROXS).<sup>24</sup> Previous studies had shown that redox blinking could be induced or suppressed by controlling the lifetime of radical ions formed via the triplet state with the aid of reducing and oxidizing agents (see Scheme 1).<sup>23,32</sup> It has been shown that some fluorophores with high electron affinity could even be switched between a bright and a dark state by inducing a photoinduced electron transfer with a reductant, yielding a metastable radical anion that could be recovered by the complementary redox reaction with an oxidant.<sup>24</sup> The common ground of these studies was that the fluorescence properties and the ability to stabilize fluorophores is closely linked to their redox potentials. Interestingly, PDI exhibits redox potentials that are in between those of recently studied dyes with  $E_{\text{ox}} \sim 1.4 \text{ V}$  and  $E_{\text{red}} \sim -0.6 \text{ V}$  versus SCE (see Scheme 1 for Jablonski diagram of PDI and approximate energy levels of the radical cation and anion).<sup>33</sup> So the electron affinity of PDI is higher than that of, for example, ATTO647N, whose fluorescence is stabilized by common redox agents, and lower than that of ATTO655. The oxazine ATTO655 exhibits blinking in the presence of a typical ROXS because the energy of the radical anion is too low to be easily reoxidized by, for example, *N,N*-methylviologen.<sup>23,24</sup> Scheme 1 also indicates that, due to the short lifetime of the singlet state, photoinduced electron transfer occurs primarily from the triplet state at the used concentration of redox agents in the micromolar range. In the following we examined the prediction of the ROXS concept that the properties of PDIs should be in between the other two prototypical fluorophores.

Figure 2A shows the PDI emission in PBS, where no considerable amplitude is observed in the autocorrelation function. Adding 1 mM *N,N*-methylviologen (MV) and 100  $\mu\text{M}$  ascorbic acid (AA) after enzymatically removing oxygen<sup>23</sup> also

(30) Vinayak, R.; Tang, H. *Nucleic Acids Symp. Ser.* **2000**, 257–258.

(31) Vosch, T.; Cotlet, M.; Hofkens, J.; Van Biest, K.; Lor, M.; Weston, K.; Tinnefeld, P.; Sauer, M.; Latterini, L.; Muellen, K.; De Schryver, F. C. *J. Phys. Chem. A* **2003**, 107, 6920–6931.

(32) Vogelsang, J.; Cordes, T.; Tinnefeld, P. *Photochem. Photobiol. Sci.* **2009**, 8, 486–496.

(33) Chengyun, W.; Wei, T.; Hanbin, Z.; Xuechao, Z.; Yongjia, S. *J. Heterocycl. Chem.* **2009**, 46, 881–885.

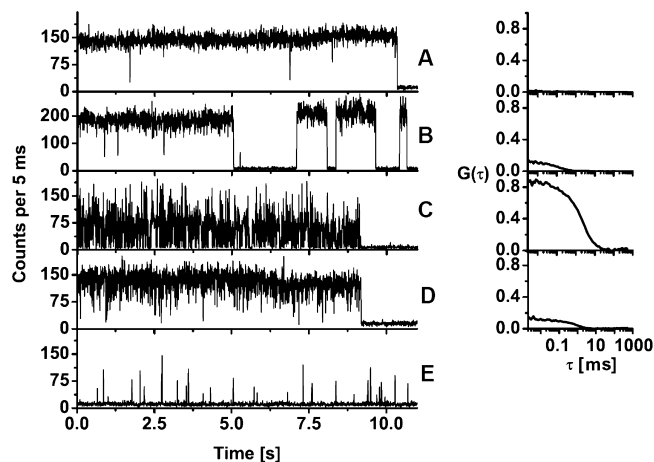


**Figure 2.** Fluorescence transients and corresponding autocorrelation functions from single immobilized dsDNA–PDI under different aqueous buffer conditions. Excitation was at 560 nm with an average intensity of  $3.8 \text{ kW/cm}^2$ . (A) PBS buffer. (B and C) ROXS buffer conditions: (B) deaerated PBS buffer with  $100 \mu\text{M}$  AA and  $1 \text{ mM}$  MV; (C) deaerated PBS buffer with  $50 \mu\text{M}$  AA and  $10 \mu\text{M}$  MV. (D and E) Reducing buffer conditions: (D) PBS buffer with  $100 \mu\text{M}$  AA; (E) deaerated PBS buffer with  $100 \mu\text{M}$  AA. Here off-times of  $500 \pm 380 \text{ ms}$  were observed. Due to the long off-time, these values were derived from on/off histograms, in contrast to panels A–D, where the given off-times were obtained by autocorrelation analysis.

yields stable fluorescence over several seconds with some long off-states (Figure 2B). A close look reveals that the signal in Figure 2B fluctuates slightly more than limited by shot noise also during the apparent on-times. This fluctuation is revealed in the autocorrelation of the data (not including the long off-states) that yields a small amplitude with on-times of  $1.6 \pm 1.1 \text{ ms}$  and off-times of  $170 \pm 100 \mu\text{s}$ . On- and off-times were determined as described previously.<sup>24</sup> We ascribe the short off-state to radical anion states. This meets the expectation under these conditions since the fluorophore with the lowest electron affinity shows no detectable off-state (ATTO647N) and the fluorophore with a higher electron affinity (ATTO655) exhibits longer off-states in the millisecond range. The fact that, in contrast to oxygen, MV is not able to quench the radical anion efficiently is in accordance with the lower reduction potential of MV compared to  $\text{O}_2$ . The longer lifetime of the radical ions in the absence of oxygen is also reflected in the photostability, because PDI emits slightly fewer photons under these conditions (average  $34\,000 \pm 8\,000$  detected photons,  $\tau_{\text{bleach}} \sim 2.9 \pm 0.9 \text{ s}$ ) than in PBS (average  $44\,000 \pm 15\,000$  detected photons,  $\tau_{\text{bleach}} \sim 2.3 \pm 0.8 \text{ s}$ ). The long off-states of up to seconds, however, cannot be explained by the model and might be related to reversible reactions visualized on the single-molecule level.<sup>34</sup>

When the amounts of AA and MV are reduced to  $50 \mu\text{M}$  and  $10 \mu\text{M}$ , respectively, blinking is more pronounced (Figure 2C) and the off-state assigned to the radical anion becomes significantly longer ( $\tau_{\text{off}} = 10 \pm 1.2 \text{ ms}$ ). This dependence on MV concentration supports our previous assignment of this state to the radical anion. The corresponding autocorrelation, however, has to be fitted by two exponentials. A second short component with  $\tau_{\text{off}} = 0.1 \pm 0.05 \text{ ms}$  can be assigned to the triplet state, which is only slowly depopulated via intersystem crossing/phosphorescence or reduction at this low reductant concentration. This assignment is also in accordance with the lifetime of

PDI triplet states determined before<sup>35</sup> and with previous findings of two components in the blinking of dyes at low ROXS concentrations.<sup>24</sup>

In the following we studied whether the achieved understanding of PDI blinking could be used for superresolution microscopy based on the subsequent localization of single molecules.<sup>4–6</sup> In order to use blinking for superresolution microscopy, the largest fraction of fluorophores has to be switched into a transient off-state at any time of the imaging process so that the remaining sparse subpopulation of molecules can be localized. Therefore, the off-state lifetime has to be long compared to the on-state lifetime. The achievable resolution is dependent on the ratio of off- to on-time.<sup>36</sup> To maximize the off-state lifetime for PDIs, we applied reductants purely to decrease the depopulation rate of the reduced state.<sup>28</sup> Therefore, fluorescence transients without the addition of external oxidants such as MV were studied. Upon addition of AA in the presence of oxygen, PDI exhibits blinking with off-times of  $\sim 1 \text{ ms}$ . The off-states are induced through reduction predominantly from the triplet state, and the off-state lifetime is determined by the oxidation potential of oxygen and its concentration. Certainly, these off-states are too short to be used for superresolution microscopy based on the subsequent localization of single fluorophores,<sup>28</sup> but they may be exploited for other high-resolution approaches that require rapid switching.<sup>37</sup> We subsequently removed oxygen enzymatically and observed longer off-states of  $500 \pm 380 \text{ ms}$  (see Figure 2E). In the corresponding transient, only short on-times are observed. The on- and off-times of this transient were determined by use of an intensity threshold and on/off histograms since the autocorrelation analysis became imprecise with such long off-times.<sup>38</sup> We assume that the recovery of the radical anion on the time scale of  $500 \text{ ms}$  is due to reaction with remaining molecular oxygen that could only be reduced down to  $\sim 13 \mu\text{M}$  by the enzymatic glucose oxidase/catalase system. Although PDI molecules were not continuously off in contrast to other fluorophores,<sup>24</sup> the dominating reduced state can be viewed as an off-state under photodynamic equilibrium.

We therefore recorded confocal images of single immobilized PDI molecules in PBS (Figure S8A in Supporting Information). As in Figure 1, diffraction-limited spots were observed. After the scan we changed to reducing conditions by adding  $100 \mu\text{M}$  AA and removing oxygen. In the next scan, no spots were observed but isolated bright pixels indicated the presence of the molecules (Figure S8B in Supporting Information). Exchanging the buffer to PBS again restored the fluorescence image (Figure S8C in Supporting Information). This procedure could be repeated several times, and two such cycles are displayed in Figure S8 (Supporting Information). The data showed that trapping of PDI in the off-state and controlling the number of emitted photons before it enters an off-state can be viewed as switching under photodynamic equilibrium. Such switching is a key ingredient for superresolution microscopy

(34) Christ, T.; Kulzer, F.; Bordat, P.; Basche, T. *Angew. Chem., Int. Ed.* **2001**, *40*, 4192–4195.

(35) Bell, T. D. M.; Habuchi, S.; Masuo, S.; Oesterling, I.; Muellen, K.; Tinnefeld, P.; Sauer, M.; van der Auweraer, M.; Hofkens, J.; De Schryver, F. C. *Aust. J. Chem.* **2004**, *57*, 1169–1173.

(36) Cordes, T.; Strackharn, M.; Stahl, S. W.; Summerer, W.; Steinhauer, C.; Forthmann, C.; Puchner, E. M.; Vogelsang, J.; Gaub, H. E.; Tinnefeld, P. *Nano Lett.* **2009** [Online early access]. DOI: 10.1021/nl903730r. Published online: December 17, 2009.

(37) Vogelsang, J.; Cordes, T.; Forthmann, C.; Steinhauer, C.; Tinnefeld, P. *Nano Lett.* **2010** [Online early access]. DOI: 10.1021/nl903823s. Published online: January 8, 2010.

(38) Yip, W. T.; Hu, D. H.; Yu, J.; Vanden Bout, D. A.; Barbara, P. F. *J. Phys. Chem. A* **1998**, *102*, 7564–7575.

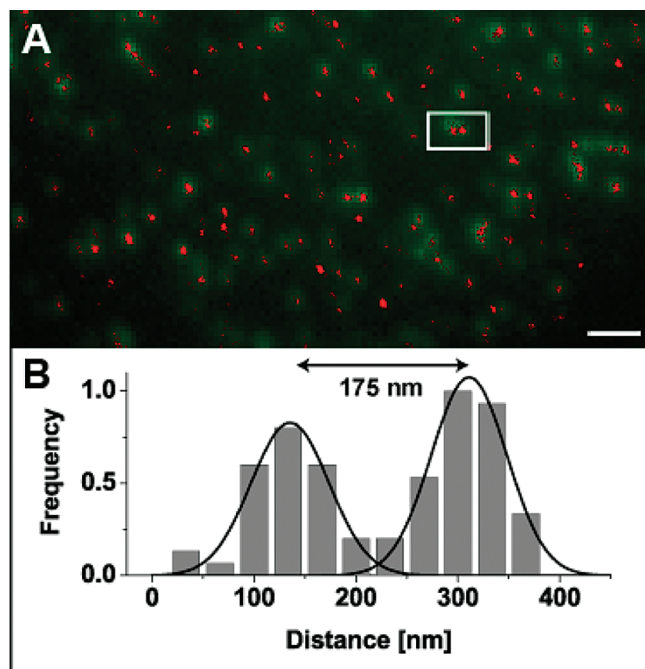


**Figure 3.** (A) Overlaid TIR fluorescent sum-image (green) and reconstructed superresolution image (red) of a densely functionalized surface of PDI molecules under reducing buffer conditions with removal of oxygen. The white scale bar is  $1 \mu\text{m}$  in length. (B) Histogram of localizations of two single molecules that were separated by a distance below the diffraction limit, that is,  $175 \text{ nm}$  (see white rectangle in panel A). The PDI molecules could be localized with a precision of  $68 \pm 24 \text{ nm}$  (value derived from several single-molecule localizations).

based on fluorescence confinement (RESOLFT concept)<sup>39</sup> or fluorescence localization.<sup>4–6</sup>

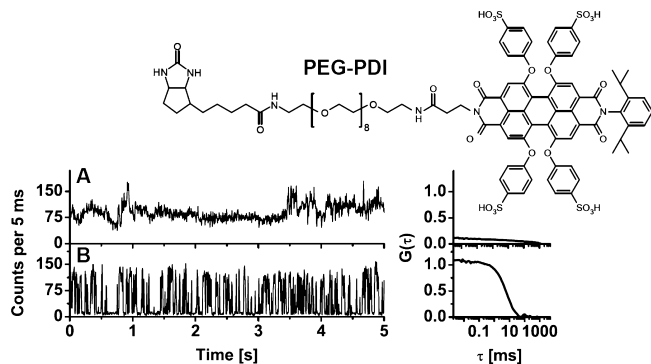
Recently, blinking molecules have been used for superresolution microscopy by subsequently localizing the fraction of fluorescent molecules.<sup>28,40,41</sup> By switching fluorophores between the on- and off-fractions, the positions of all fluorophores are determined successively, and reconstructed images that are not limited by diffraction are generated.<sup>4</sup> A proof-of-principle experiment was conducted by immobilizing single PDI dyes with a density above 1 fluorophore/PSF on a cover slide and by manipulating their emission in a reducing buffer. Application of  $12 \mu\text{M AA}/2 \mu\text{M MV}$  with removal of oxygen allowed us to localize the molecules even on a surface where overlapping emission was registered in the TIR fluorescent images (Figure 3). The exact procedure and image reconstruction of “Blink-Microscopy” are described in Supporting Information and in refs 24 and 28.

Figure 3 shows a TIR fluorescent image (green) of a densely functionalized surface of PDI molecules overlaid with a reconstructed superresolution image (red). The localization events from “Blink-Microscopy” within the white rectangle (Figure 3A) were projected onto the horizontal axis and the corresponding histogram is displayed in Figure 3B. Here, subdiffraction resolution was demonstrated with a distance of  $175 \text{ nm}$  between two single emitters. On average  $100 \pm 60$  on-counts per fluorescent cycle were obtained, leading to an experimental localization precision of  $68 \pm 24 \text{ nm}$ , obtained

(39) Hell, S. W. *Science* **2007**, *316*, 1153–1158.

(40) Folling, J.; Bossi, M.; Bock, H.; Medda, R.; Wurm, C. A.; Hein, B.; Jakobs, S.; Eggeling, C.; Hell, S. W. *Nat. Methods* **2008**, *5*, 943–945.

(41) van de Linde, S.; Kasper, R.; Heilemann, M.; Sauer, M. *Appl. Phys. B: Lasers Opt.* **2008**, *93*, 725–731.



**Figure 4.** Structure and fluorescent transients with corresponding auto-correlation analysis from confocal microscopy of a PDI derivative immobilized in the organic solvent acetonitrile. Excitation intensity was  $0.6 \text{ kW}/\text{cm}^2$  at  $560 \text{ nm}$ . (A) Data in acetonitrile with intensity fluctuations on various time scales but no distinct blinking (see autocorrelation analysis in the right panel). (B) Data in acetonitrile with additional  $100 \mu\text{M AA}$ . In the trace shown, on-times of  $15 \text{ ms}$  with  $255$  on-counts and off-times of  $16 \text{ ms}$  were determined by autocorrelation analysis (see right panels). The blinking is attributed to transitions into a reduced nonfluorescent form of the PDI molecule.

from repeated localization of the same molecule with the error representing the standard deviation from the localization precision of different molecules. Theoretically, a localization precision of  $39 \text{ nm}$  was expected,<sup>42</sup> and we ascribed the deviation from the experimental value to imperfection of the experimental setup (background noise, thermal drift,  $\sim 13 \text{ nm}$  length of the PDI linker). As has been shown for ATTO655, the number of on-counts and off-times can be adapted by the concentration of redox-active agents.<sup>24</sup> This will allow a trade-off of spatial versus temporal resolution.<sup>36</sup>

The presented data (Figure 3) demonstrate that PDI dyes are suitable as labels for recording images with subdiffraction resolution. Consideration of their superior photostability in hydrophobic media and organic solvents suggests that they should be ideal candidates for subdiffraction imaging under these conditions. To test whether the photophysics of PDI could be manipulated similarly in nonaqueous conditions, we immobilized a PDI linked via a poly(ethylene glycol) (PEG) linker (see Figure 4) to BSA/BSA–biotin in acetonitrile. Interestingly, the immobilization was stable even under these conditions. In acetonitrile, the PDI molecules were significantly brighter and similar fluorescence count rates were obtained at lower excitation intensities of  $0.6 \text{ kW}/\text{cm}^2$  (Figure 4A). Importantly, redox blinking was also induced upon the addition of AA to the immobilized molecules in acetonitrile (Figure 4B). For 20 molecules, mean off-times of  $8 \pm 4 \text{ ms}$  and on-times of  $13 \pm 8 \text{ ms}$  were measured with an average of  $200 \pm 110$  detected photons per on-time.

In conclusion, the photophysics of single water-soluble PDI, an important member of rapidly emerging rylene dye biolabels, was studied under aqueous conditions for the first time. Our results indicate that PDIs are suited for a wide range of applications in single-molecule fluorescence spectroscopy and superresolution microscopy. All results could be explained on the basis of the ROXS concept and with knowledge of the electronic properties of the PDIs. The high electron affinity easily enabled the induction of redox blinking to metastable

(42) Bossi, M.; Folling, J.; Belov, V. N.; Boyarskiy, V. P.; Medda, R.; Egner, A.; Eggeling, C.; Schonle, A.; Hell, S. W. *Nano Lett.* **2008**, *8*, 2463–2468.

radical anion states, while no evidence for radical cation states was found. Interestingly, the PDIs were most photostable in the presence of oxygen since oxygen is an efficient quencher of the radical anion state (more efficient than MV). Taking into account that oxazine fluorophores, which also exhibit a high electron affinity, are similarly photostable in the presence of oxygen, this seems to be a common feature of “oxygen-resistant” fluorophores.<sup>24,27</sup>

In summary, the redox properties are one of the most important characteristics of single-molecule-compatible fluorescent dyes. Since the redox potentials of PDIs can be well adapted by chemical substituents, they could be well designed for single-molecule applications requiring stable emission in ROXS by decreasing their electron affinity. On the other hand, superresolution “Blink-Microscopy” might be possible in the presence of oxygen if the electron affinity were increased to a level where the radical anion was not effectively depopulated

through reaction with molecular oxygen.<sup>24</sup> This, in combination with their tunable solubility properties from organic solvents to aqueous medium and their variable functionalizability, strongly points toward their broad applicability in the rapidly growing field of single-molecule fluorescence spectroscopy.

**Acknowledgment.** We are grateful to Christian Steinhauer and Carsten Forthmann for help with data analysis and fruitful discussions. This work was supported by the DFG (Inst 86/1051-1), the Biophotonics Program of the BMBF/VDI, the Nanosystems Initiative Munich, and the Elitenetzwerk Bayern.

**Supporting Information Available:** Experimental methods and additional data as described in the text. This material is available free of charge via the Internet at <http://pubs.acs.org>.

JA9099714